Published manuscript at **https://doi.org/10.1098/rsfs.2019.0123**

Applicability assessment of a stent-retriever thrombectomy finite-element model

Giulia Luraghi[1], Jose Felix Rodriguez Matas[1], Gabriele Dubini[1], Francesca Berti[1], Sara Bridio[1], Sharon Duffy[2], Anushree Dwivedi[2], Ray McCarthy[2], Behrooz Fereidoonnezhad[3], Patrick McGarry[3], Charles B.L.M. Majoie[4], Francesco Migliavacca[1]; on behalf of the INSIST investigators*

[1] "Department of Chemistry, Materials and Chemical Engineering 'Giulio Natta', Politecnico di Milano, Milan, Italy.
[2] Cerenovus, Galway Neuro Technology Center, Galway, Ireland.
[3] Department of Biomedical Engineering, National University of Ireland Galway, Galway, Ireland.
[4] Departments of Radiology and Nuclear Medicine, Academic Medical Center, Amsterdam, the Netherlands.
* The INSIST investigators are given in the Appendix

Corresponding author:
Giulia Luraghi
Laboratory of Biological Structure Mechanics (LaBS)
Department of Chemistry, Materials and Chemical Engineering "Giulio Natta", Piazza L. da Vinci 32, 20133 Milan, Italy.
E-mail: giulia.luraghi@polimi.it

Keywords: INSIST, thrombectomy, acute ischemic stroke (AIS), stent-retriever, finite element analysis (FEA)

Published manuscript at **https://doi.org/10.1098/rsfs.2019.0123**

Abstract

An acute ischemic stroke (AIS) appears when a blood clot blocks the blood flow in a cerebral artery. Intra-arterial thrombectomy, a mini-invasive procedure based on stent technology, is a mechanical available treatment to extract the clot and restore the blood circulation. After stent deployment, the clot, trapped in the stent struts, is pulled along with the stent towards a receiving catheter. Recent clinical trials have confirmed the effectiveness and safety of the mechanical thrombectomy. However, the procedure requires further investigation. The aim of this study is the development of a numerical finite element-based model of the thrombectomy procedure. *In vitro* thrombectomy tests are performed in different vessel geometries and one simulation for each test is carried out to verify the accuracy and reliability of the proposed numerical model. The results of the simulations confirm the efficacy of the model to replicate all the experimental setups. Clot's stress and strain fields from the numerical analysis, which vary depending on the geometric features of the vessel, could be used to evaluate the possible fragmentation of the clot during the procedure. The proposed in vitro/in silico comparison aims at assessing the applicability of the numerical model and at providing validation evidence for the specific in vivo thrombectomy outcomes prediction.

1. Introduction

An acute ischemic stroke (AIS) occurs when an artery that supplies blood to the brain is blocked by a blood clot (thrombus), which is a solidified mass of blood cells, platelets, fibrin, and other blood components occurring as a result of blood coagulation. Rarely, occlusive clots may also consist of non-thrombus components such as fat emboli, tumor tissue, calcifications and the like. In the majority of AIS cases the clot is formed elsewhere and embolized to the vessel it eventually occludes, although in situ occlusive thrombi also occur. Red thrombi, red blood cell (RBC) dominant, are understood to form where the blood flow is slow and the fibrin network entraps the RBCs, while white thrombi, fibrin dominant, are generated under high shear flow and inflammatory conditions [1]. Mechanical properties of blood clot strongly depend on the clot composition [1]. Common origins of embolic thrombi are the heart, atherosclerotic plaques, or from vessel wall dissections.

Detection of the location of the intracranial occlusion must be done in a fast and accurate way to ensure an appropriate selection of treatment and its speedy delivery [2]. Treatment of AIS is aimed at restoring blood flow in the affected cerebral arteries as quickly as possible. *Time is crucial in stroke*- 2 million neurons are lost every second without reperfusion [3]. The main diagnostic imaging techniques used to identify the clot location are computed tomography (CT) and magnetic resonance imaging (MRI).

There are currently two main therapies to treat an ischemic stroke: i) medical therapy using thrombolytic agents (thrombolysis) and ii) interventional therapy to remove the clot using mechanical thrombectomy. The latter being indicated for large vessel occlusions of the neurovasculature. Thrombolysis became available recently and involves the administration of tissue plasminogen activator 3-4.5 hours after the onset of a stroke. Most recently, intra-arterial mechanical thrombectomy has emerged as a widespread clinical intervention technique in the treatment of stroke [4]. Currently, a combined approach of thrombolysis and mechanical thrombectomy is recommended

for the treatment of AIS involving large vessel occlusion. Mechanical thrombectomy interventions are carried out with the aid of angiography to ensure the correct positioning of the devices relative to the occluded vessel.

Thrombectomy device design has two classifications based on their mode of action, (i) aspiration catheters and (ii) stent-retrievers. Aspiration catheters may be used without stent retrievers; however, stent retriever use usually includes some element of aspiration, either through a guide catheter placed in the extracranial internal carotid artery (ICA) or using a distal access catheter which can be placed close to the occlusion in smaller intracranial vessels. Superiority of one approach over the other is an ongoing subject of debate amongst neurointerventionalists [5–7]. Effectiveness of the thrombectomy approach taken is measured in terms of speed of revascularization, reperfusion grade, patient outcome, ease-of-use, and cost of procedure. The revascularization of the affected vessels is strongly associated with improved clinical outcomes for patients [8].

Stent retrievers rely on the mechanical removal of the thrombus by means of a Nickel-Titanium (NiTi) self-expandable stent at the end of a flexible wire, delivered in a crimped configuration in a microcatheter and positioned across the thrombus. Once in position, the stent-retriever is deployed by withdrawing the microcatheter (even at this stage, the expanded stent may restore the blood flow by compressing the clot between the stent-retriever and the arterial wall). After deploying the stent-retriever, the clot, trapped in the stent struts, is pulled along with the stent towards a receiving catheter. In many cases, this operation is performed under arrested flow conditions achieved by a balloon inflated in a guide catheter positioned at the ICA at the skull base. A number of stents-retriever device designs are currently being used in clinical practices [9], and a number of clinical trials are currently ongoing [8,10–12]. In this regard, the seminal MR CLEAN clinical trial [13], a multicenter randomized clinical trial of endovascular treatment (EVT) for AIS in the Netherlands, confirmed the effectiveness and safety of stent-retriever thrombectomy devices and demonstrated their improved outcome when combined with best medical therapy compared to thrombolysis alone.

However, despite its increasing clinical application, thrombectomy may result in some adverse outcomes, such as thrombus embolization to distal vessels caused by disruption of the clot during crossing, deployment or retrieval [14], embolization of clot to new vascular territories, hemorrhagic events, and vessel wall damage [15,16]. Procedural success also greatly depends on vascular geometry (tortuosity), clot characteristics, or in cases involving atherosclerotic stenosis [6].

To date, a limited number of *in vitro* and *in silico* studies on the thrombectomy procedure have been reported. *In vitro* studies have investigated the mechanical behavior and functioning of devices [17] and clots [18], and the stent-clot interaction [19,20]. In the few published *in silico* studies [21,22], the procedure was modeled as an electric circuit analog and the clot as a spring-damper system, ignoring the mechanical nature of the stent-clot interaction.

In this regard, the increasing fascination of performing “virtual” treatment in “virtual” patients [23] makes necessary the development of accurate *in silico* models of the thrombectomy procedure. An *in silico* clinical trials of AIS incorporating a robust *in silico* thrombectomy model would enable evaluation of various hypotheses on the effectiveness of thrombectomy. *In silico* thrombectomy models in numerous vessel geometries and with different clot characteristics would allow rapid

evaluation of the feasibility of different thrombectomy treatment approaches for specific patients, and patient populations, resulting in faster and safer introduction of new treatments or devices.

In this context, the objective of the current study is to develop an *in silico* finite-element model of the thrombectomy procedure and to demonstrate the ability of the model to replicate experimental thrombectomy tests using commercial stents-retriever and clot analogs. To the best of our knowledge, this is the first finite element model of the thrombectomy procedure. *In vitro* tests are also performed to verify the accuracy and reliability of the numerical models. The proposed *in vitro/in silico* comparison aims at assessing the applicability of the numerical model and at providing validation evidence for the specific in vivo thrombectomy outcomes prediction, which constitutes the ultimate *Context of Use* (COU). In particular, finite element models of the stent-retriever and the clot are developed and their mechanical behavior is calibrated with experimental tensile and compression tests; *in vitro* bench-top tests in different cerebral-like vessel geometries (idealized and anatomically-based), are performed - and a computational simulation of each in *vitro* test is implemented using the *in silico* thrombectomy modeling framework.

2. Method

2.1 Stent-Retriever model

The EmboTrap II (CERENOVUS, Galway, Ireland) is a NiTi stent-retriever with a dual-layer design (Fig. 1a): the outer stent cage has large openings aimed at trapping the clot, while articulating leaflets maintain the contact with the arterial wall during retrieval, the inner channel formed by a closed-cell stent is aimed at trapping captured clot within the stent-retriever and restoring the blood flow through the clot upon deployment [24]. The device was approved for the use in EU in late 2013 under the CE mark. The CAD model (5mm outer diameter and 33mm length) was analyzed by means of ANSA Pre Processor v19.0 (BETA CAE System, Switzerland) to extract the centerline of the frames (Fig. 1b). The resulting wire model was discretized with 4,353 Hughes-Liu beam elements with rectangular cross section and average length 0.2 mm, following a rigorous mesh size sensitivity analysis. In particular, three different discretizations with average element size of 0.4 mm, 0.2 mm and 0.1 mm were considered, with the resultant force and the axial stresses on selected elements in the central part of the device used as monitored variables for the convergence analysis. The difference in the monitored variables between the 0.2mm and the 0.1 mm discretization was less than 3 % during the crimping step of the simulations. The stent's cross sections were measured with a confocal laser scanning microscope (LEXT-OLS4100, Olympus) (Fig. 1c). A self-penalty hard contact between the struts of the stent was modeled in order to prevent inter-penetration of the inner parts of the retriever during the simulations.

The NiTi material parameters, provided by CERENOVUS (data not shown), were verified through a numerical-experimental coupling [25]: the stent was subjected to a uniaxial tensile test at an applied displacement rate of 0.05 mm/min until its length is extended by 4.5 mm, in a temperature-controlled chamber with air at 37.0±0.1°C (EnduraTEC ELF 3200, BOSE) (Fig. 1d). The experiment was then computationally simulated (Fig. 1e) and the NiTi material was modeled using the shape memory material constitutive formulation available in the commercial finite element solver LS-DYNA 971

Release 11.0 (ANSYS, Canonsburg, PA, USA) [26].

Crimping simulations of the device in a microcatheter with an inner diameter of 0.5 mm followed by unconstrained release, were carried out to verify the crimping and release kinematic of the device. These simulations were used to determine the optimal system damping and mass scaling [27]. Internal, kinematic and dissipative energies were compared in order to guarantee quasi-static conditions during the simulation i.e., a kinetic to internal energy ratio of less than 2 %. The finite element simulations were performed on 16 CPUs of an Intel Xeon64 with 64 GB of RAM memory using the commercial finite element solver LS-DYNA 971 Release 11.0 (ANSYS, Canonsburg, PA, USA).

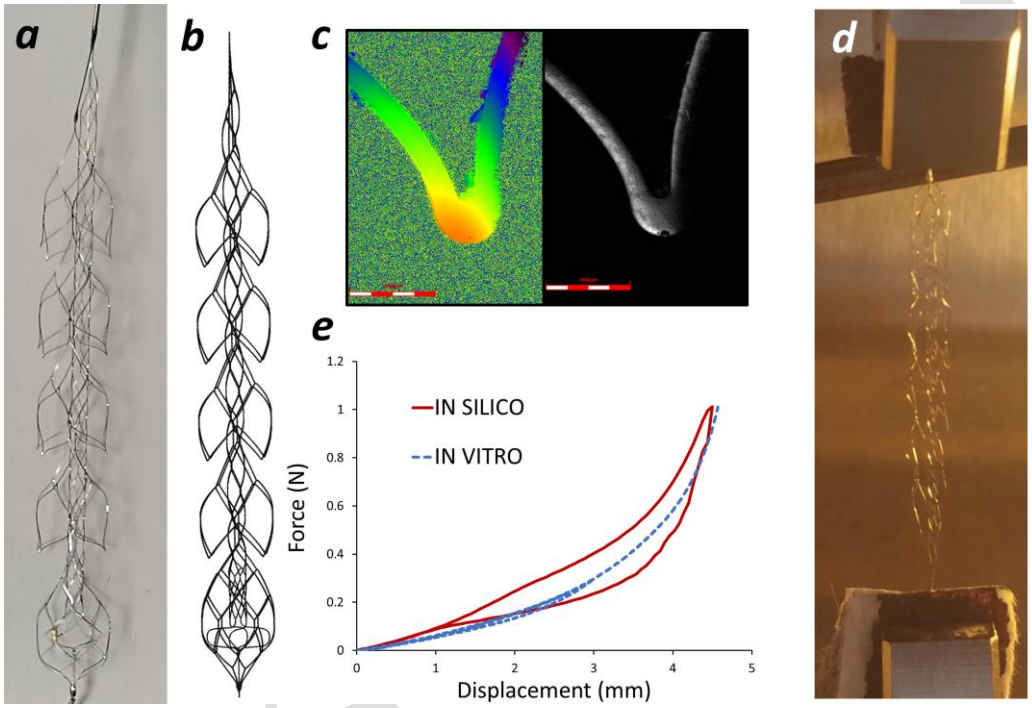

Figure 1: (a) EmboTrap II device and (b) its finite element model, discretized with beam elements; (c) the stent section acquired with the confocal laser scanning microscope; (d) uniaxial tensile test and (e) the resultant force-displacement curve (dotted blue line), compared with the curve from the in silico model (solid red line).

2.2 Clot model

Clots analogs were obtained from venous whole ovine blood using a customized protocol [28,29] (Fig. 2a). Unconfined compression tests of synthetic clots in 0.9% saline were performed using a custom-built parallel plate experimental (Fig. 2b). Clots with a composition intermediate between red and white clots (ca. 20% RBC) were subjected to confined compression up to 80 % nominal compressive strain at an applied strain rate of 10% s^{-1}. The compressibility of the blood clot was also investigated by processing of the images taken at different deformations during the compression test. The initial deformation of the clot at the start of the test leads to the calibration of a Poisson's ratio of 0.3.

The compression test was numerically reproduced using a simplified quasi hyperelastic foam model defined by a single uniaxial load curve and an assumed Poisson's ratio [30]. The term quasi is used

because there is really no strain energy function for determining the stresses. In this regard, the stress response mimics the gradient of the classical Hill-Ogden strain energy potential which for the case of a foam reads

$$\tau_{ii}^{E} = f(\lambda_i) - f\left(J^{-\frac{\nu}{1-2\nu}}\right),$$

where τ_{ii}^{E} are the principal components of the Kirchhoff stress, ν is the Poisson's ratio, λ_i the principal stretches, with $J = \lambda_1\lambda_2\lambda_3$ the relative volume change, and $f(.)$ a function determined directly from uniaxial test data as [30]:

$$f(\lambda) = \lambda g(\lambda) + \lambda^{-\nu} g(\lambda^{-\nu}) + \cdots + \lambda^{(-\nu)^n} g\left(\lambda^{(-\nu)^n}\right),$$

where $\tau = g(\lambda)$ corresponds to the experimental uniaxial curve. The formulation does not require an analytical expression for $f(.)$, this function consists on tabulated values of the principal stretch ratios and the input Poisson's ratio. The tabulated values are determined by LS-DYNA at the beginning of the computation in such a way that supplied data from uniaxial tension and compression tests are fitted within an arbitrarily small error, whereas linear interpolation is used to approximate the function between tabulated values. Figure 2c shows the performance of the model to replicate the unconfined compression tests.

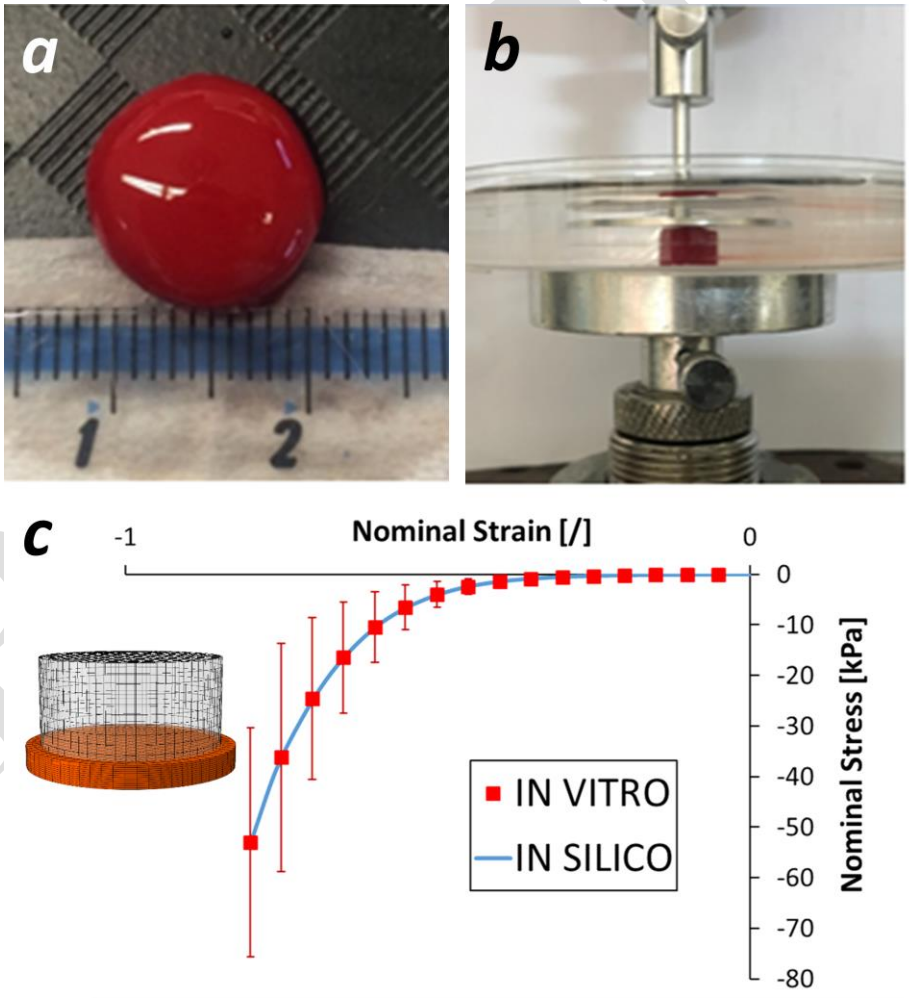

Figure 2: (a) Clots analogs from venous whole ovine blood; (b) unconfined compression test in saline solution; (c) the measured nominal stress-strain curve with standard deviation (dotted red line), compared with the curve from the *in silico* model (solid blue line).

2.3 In vitro thrombectomy tests

Three different functional bench tests were designed: i) a glass U-bent vessel; ii) a silicone funnel-shaped vessel and iii) a patient-like 3D-printed silicone vascular branch. Vessel models were fabricated with physiological dimensions in order to realistically replicate the thrombectomy procedure. Clots with the same composition (ca 20%RBC) but different sizes were used. Figure 3 shows the dimensions of the different vessel models and clots considered in the study. The experiments were carried out with a stationary flow of saline solution heated at 37°C and each procedure was video recorded. Each test was performed three times in order to assure the repeatability of the outcomes.

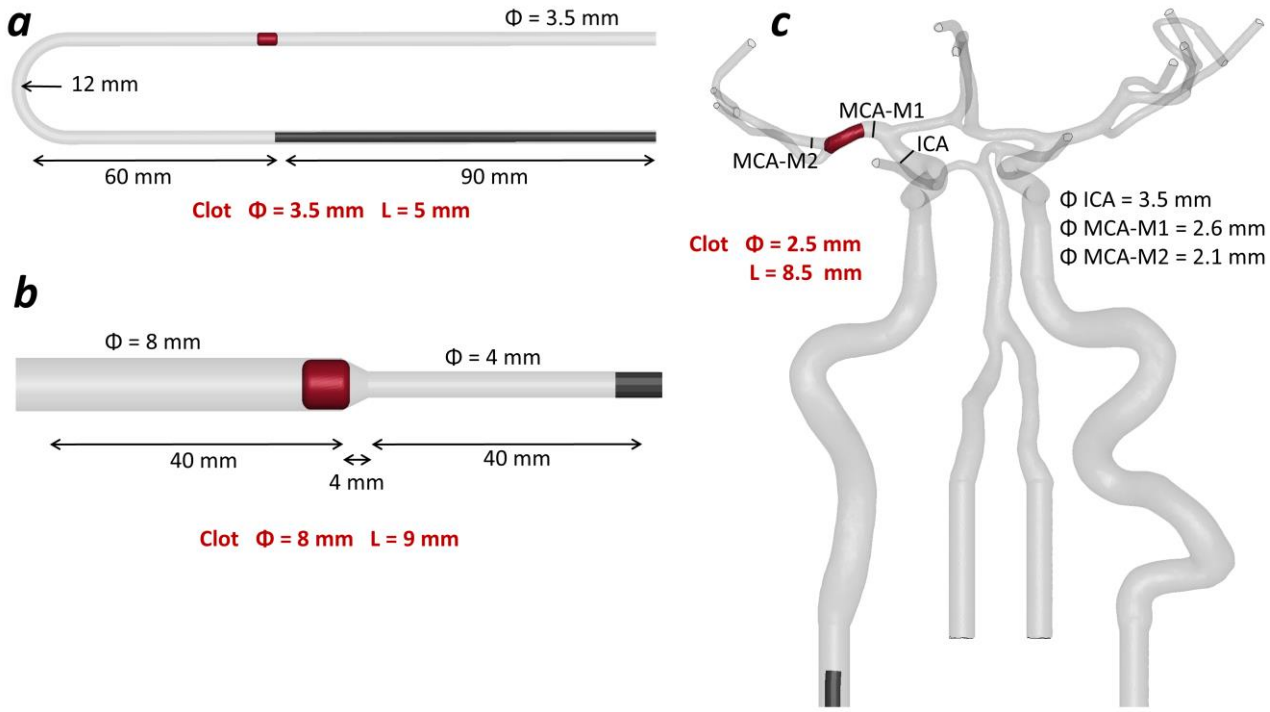

Figure 3: Geometry and dimensions of the three functional bench tests, (a) a glass U-bent vessel (b) a silicone funnel-shaped vessel and (c) a patient-like 3D-printed silicone vascular branch. Clots' diameters and lengths are also pointed out (in red).

2.4 In silico thrombectomy tests

Different clot model geometries were generated in accordance with the dimensions of the tested clot analogs. Clot model geometries were discretized with tetrahedral elements with an average size of 0.2 mm. The mesh size for the clot was chosen to be similar to that of the stent to achieve optimal simulation of the contact between the stent and the clot. A mass proportional damping of 10 s-1 was adopted for the clot in order to achieve stability without excessively constraining the maximum time step [27]. The CAD models of the glass and silicone vessels were discretized with triangular rigid elements. The clots were positioned in the vessels at the same location as the *in vitro* tests. A selective mass-scaling was adapted in order to have a constant time-step of $5 \cdot 10^{-7}$ s.

The finite element models were set-up in ANSA Pre Processor v19.0 (BETA CAE System,

Switzerland) and the simulations were performed on 40 CPUs of an Intel-Xeon64 with 256 GB of RAM memory using the commercial finite element solver LS-DYNA.

The simulation of the thrombectomy procedure consisted of four steps:

(i) *stent crimping/catheter tracking* - the stent-retriever is crimped in a 0.5 mm diameter rigid straight catheter in 1 s. A hard penalty contact is defined between the stent and the catheter; at the same time, the clot is deformed and pushed against the vessel wall by the catheter. Frictionless soft penalty contact is defined between the clot and the catheter, whereas a rough soft penalty contact is defined between the clot and the vessel wall, with a friction coefficient of 0.1 in the glass vessel and of 0.2 in the silicone vessels [31];

(ii) *stent tracking*- the crimped stent is positioned at the location of the clot by removing it along the centerline of the guide catheter at a velocity of 0.1 m/s.

(iii) *deployment* - the stent is released/unsheathed by sliding the crimping catheter from the stent at a velocity of 0.1 m/s. As the stent is released it comes into contact with the clot; a soft penalty contact is defined between the stent and the clot, whereas a hard contact is implemented where the stent contacts the rigid vessel wall.

(iv) *retrieval* - the clot trapped by the stent following release, and the stent and trapped clot are then pulled at a velocity of 0.05 m/s along the catheter's centerline until an aspiration catheter is reached.

3. Results

Simulation of the crimping of the device in the catheter followed by an unconstrained release was carried out to verify the crimping and release kinematics predicted by the model. The stent model was successfully crimped in 1 s in a 0.5 mm – diameter catheter without distortion of the beam elements, element interpenetration or instability. In Fig. 4 the simulation of the crimping is compared against the actual crimping of the Embo Trap II device. The unconstrained release in 1 s was also successfully modeled, the stent recovered its nominal open configuration with no residual stresses or strains. The quasi-static condition in this simulation was achieved, a mass-weighted damping factor for the stent of 50 s-1 and a constant time-step of $5 \cdot 10^{-7}$ s with selective element mass-scaling were identified as optimum parameters.

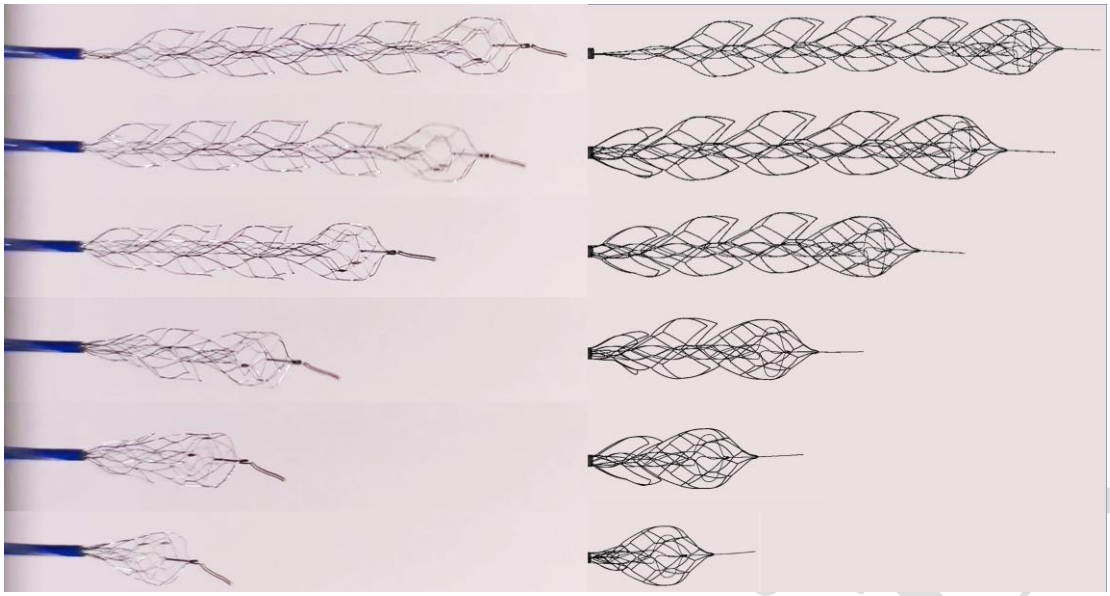

Figure 4: Comparison between the real (left panel) and the modeled (right panel) crimping phase of the device in the microcatheter with an inner diameter of 0.5 mm.

Thrombectomy in vitro tests were performed and numerically reproduced. Comparison in terms of the kinematics (structure deformation) was performed, focusing in particular on the clot's position, deformation and motion. Evaluation over time of the von Mises (VM) stresses and Green von Mises (VM) strains, also known as Effective stress and strain respectively, of the clot during all the steps of the simulations was performed. Maximum stress and strain are reported as the average of the 10 elements with the maximum value, instead of local maximum values to avoid possible spikes due to the contact of the clot with the stent or due to excessive distortion of the mesh.

The first test was conducted in a glass U-bent vessel, with a positive thrombectomy outcome. The model consisted of 48,655 finite elements and the simulation lasted 17 hours. The clot, trapped into the stent's struts, was retrieved along the bend of the vessel (Fig. 5-left panel). In this case the simulation successfully replicated the procedure (Fig. 5-right panel): during the first step (stent crimping/catheter tracking) the stent was crimped and the catheter, following the centerline of the U-bent vessel, was positioned across the cot. At this point (T_1 in Fig. 6) the clot, pushed against the vessel wall, reached a maximum VM stress of 0.6 kPa and a VM strain of 0.25. In the stent tracking phase, the crimped stent was positioned across the clot following the centerline of the catheter, while nothing occurred on the clot, whose stress and strain values remained stable. In the deployment step, the stent was released by unsheathing the catheter. As the stent and the clot enter in contact, the stress and strain values increased in the clot increase dramatically. The maximum VM stress and strain once the stent was completely released (T_2 in Fig. 6) were 36.3 kPa and 0.72, respectively. In the third and final retrieval step, the clot is trapped between the inner and the outer layer of the stent and was retrieved following the centerline of the catheter. During the retrieval phase, the maximum effective stress and strain in the clot decreased as the retriever pass the U-bent to further stabilize at a constant value as the retriever reach the straight part of the vessel. In this setting, the maximum effective stress and strain in the clot resulted in 36.5 kPa and 0.78, respectively (Fig. 6).

Figure 5: Comparison between the *in vitro* (left panel) and the *in silico* (right panel) thrombectomy test in the glass U-bent vessel. In both the results the clot, trapped in the stent, is successfully retrieved until reaching the aspiration catheter.

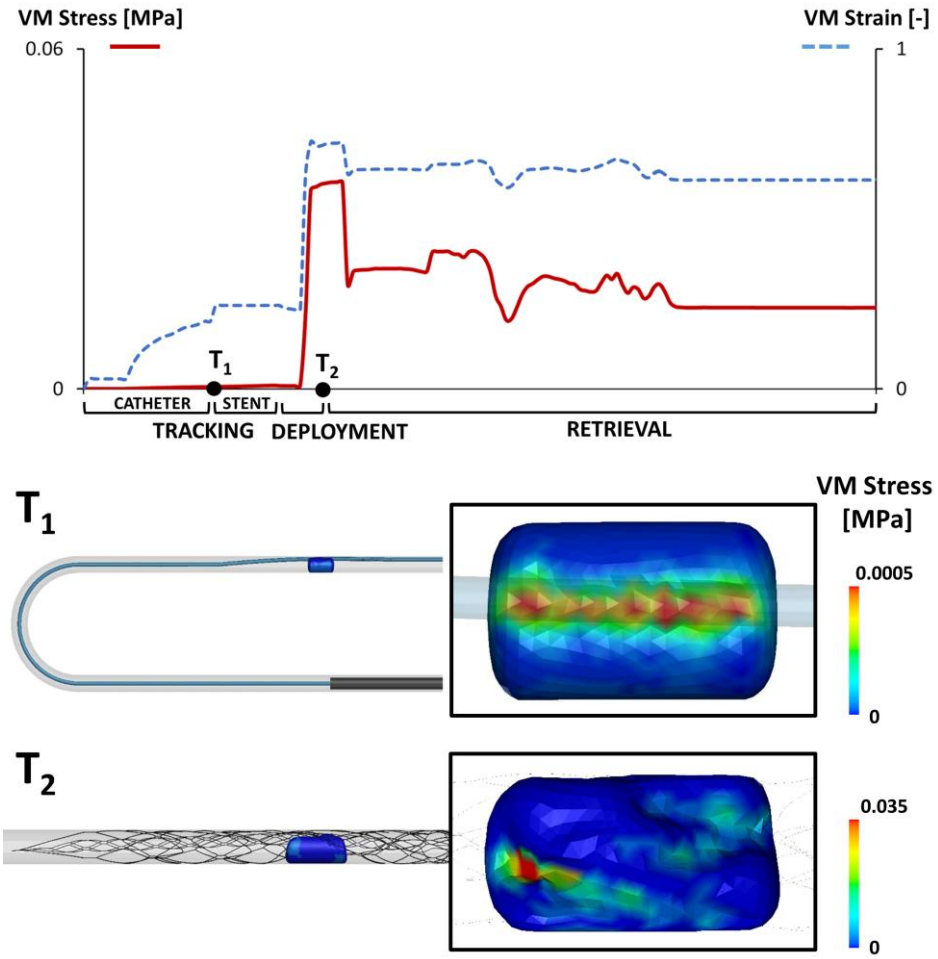

Figure 6: Maximum (averaged over 10 elements with the maximum values) von Mises (VM) stress and Green von Mises (VM) strain values over time during the *catheter tracking*, *stent tracking*, *deployment* and *retrieval* steps of the simulation in the glass U-bent vessel. von-Mises stress contours on the clot in two different views at the end of the *catheter tracking* step (time T_1) and at the end of the *deployment* step (time T_2).

The second test was conducted in a silicone funnel-shaped vessel, with a negative thrombectomy outcome. The model consisted of 50,518 finite elements and the simulation lasted 18 hours. In this case, the clot is not trapped within the retriever's struts during the retrieval phase and the retriever is unable to pull the clot through the small vessel. Instead, the clot roll up in the place where the larger vessel narrows (Fig. 7-left panel). The simulations, again, successfully replicated the (Fig. 7-right panel) too. After the first stent crimping/catheter tracking step (T_1 in Fig. 8) the clot was pushed against the vessel wall reaching a maximum VM stress of 0.4 kPa and a VM strain of 0.23, values that were maintained during the second step. During the deployment step the stent went in contact with the clot, increasing the maximum effective stress and strain values to 4.3 kPa and 0.45, respectively (T_2 in Fig. 8). In the retrieval step, the clot, due to the significantly larger vessel to retriever diameter ratio that prevented an effective clot-stent interaction, started to roll up preventing the retriever to pull the clot into smaller vessel. In this step, the continuous rolling of the clot produced oscillating values of the effective stressed and strains with peaks of 15.4 kPa and 0.61, respectively.

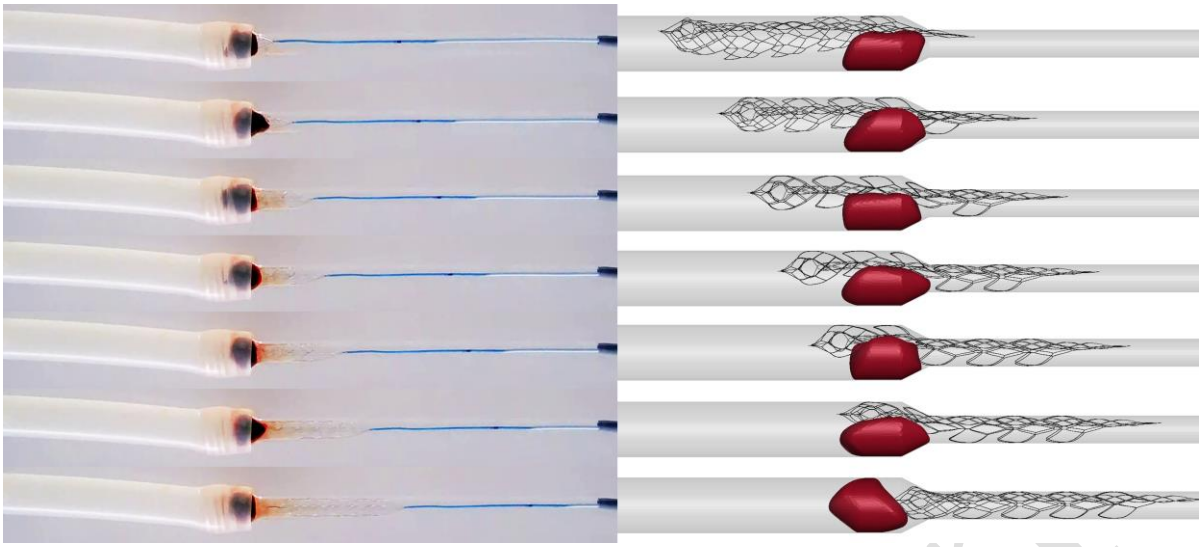

Figure 7: Comparison between the *in vitro* (left panel) and the *in silico* (right panel) thrombectomy test in the silicone funnel-shaped vessel. In both the results, the clot escaped from the stent by turning on itself.

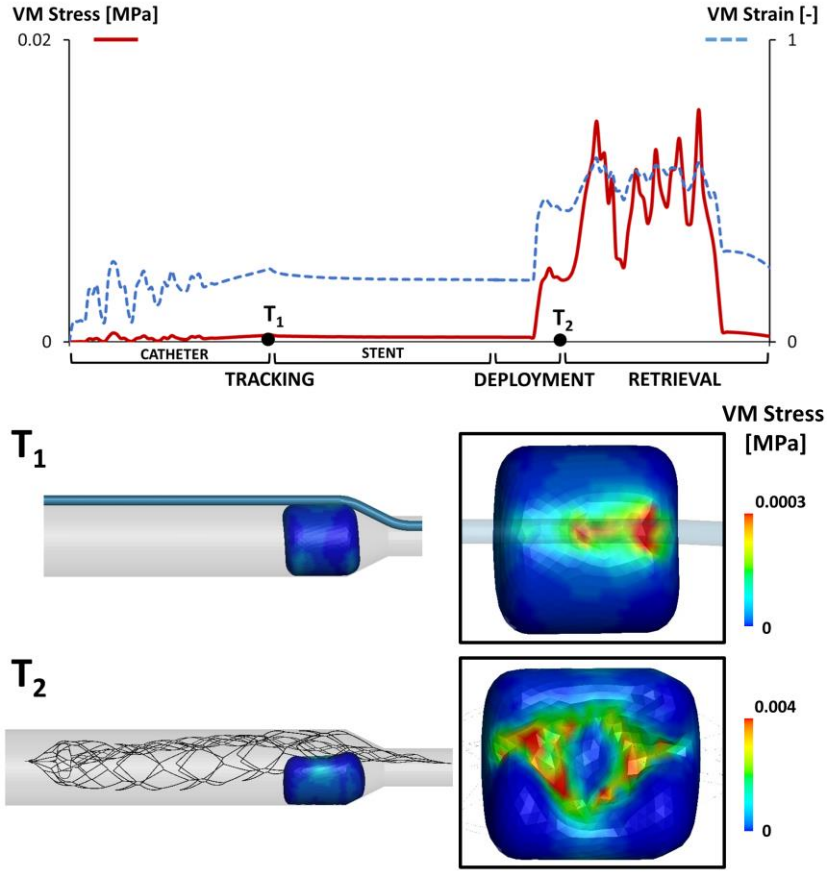

Figure 8: Maximum (averaged over 10 elements with the maximum values) von Mises (VM) stress and Green von Mises (VM) strain values over time during the *catheter tracking*, *stent tracking*, *deployment* and *retrieval* steps of the simulation in the silicone funnel-shaped vessel. von-Mises stress contours on the clot in two different views at the end of the *catheter tracking* step (time T_1) and at the end of the *deployment* step (time T_2).

The third thrombectomy test was conducted in a patient-like 3D-printed silicone vascular branch, with a positive outcome (Fig. 9-left panel). This last test is closer to the in vivo thrombectomy procedure. From a numerical point of view, the simulation was composed of the same four steps, but the tortuosity of the vessel increased the overall complexity of the solution. The model consisted of 144,760 finite elements and the simulation lasted 26 hours. This simulation demonstrates the robustness of the thrombectomy numerical model as it successfully replicated the experiments in terms of the successful retrieval (Fig. 9-right panel). In the stent crimping/catheter tracking step (T_1 in Fig. 10) the clot was pushed against the vessel wall reaching a maximum effective stress of 8.0 kPa and a maximum effective strain of 0.56, values that were maintained during the second step. During the deployment step the stent went in contact with the clot, increasing the maximum effective stress and strain values to 230 kPa and 1.02, respectively (T_2 in Fig. 10). As evidenced by these results, during the deployment phase of the retriever the clot undergoes large deformations and the stresses reach values way superior to those found in the other two experimental setups. During the retrieval phase, the clot remained trapped in the stent's struts all the way along the vessel. In this case, the open architecture of the EmboTrap II stent helped the insertion of the clot inside the stent struts [28]. During this final step, the effective stress and strain reached a maximum value of 320 kPa and 1.6, respectively.

Figure 9: Comparison between the *in vitro* (left panel) and the *in silico* (right panel) thrombectomy test in the silicone patient-like 3D-printed vascular branch. In both the results the clot, trapped in the stent, is successfully retrieved until reaching the aspiration catheter.

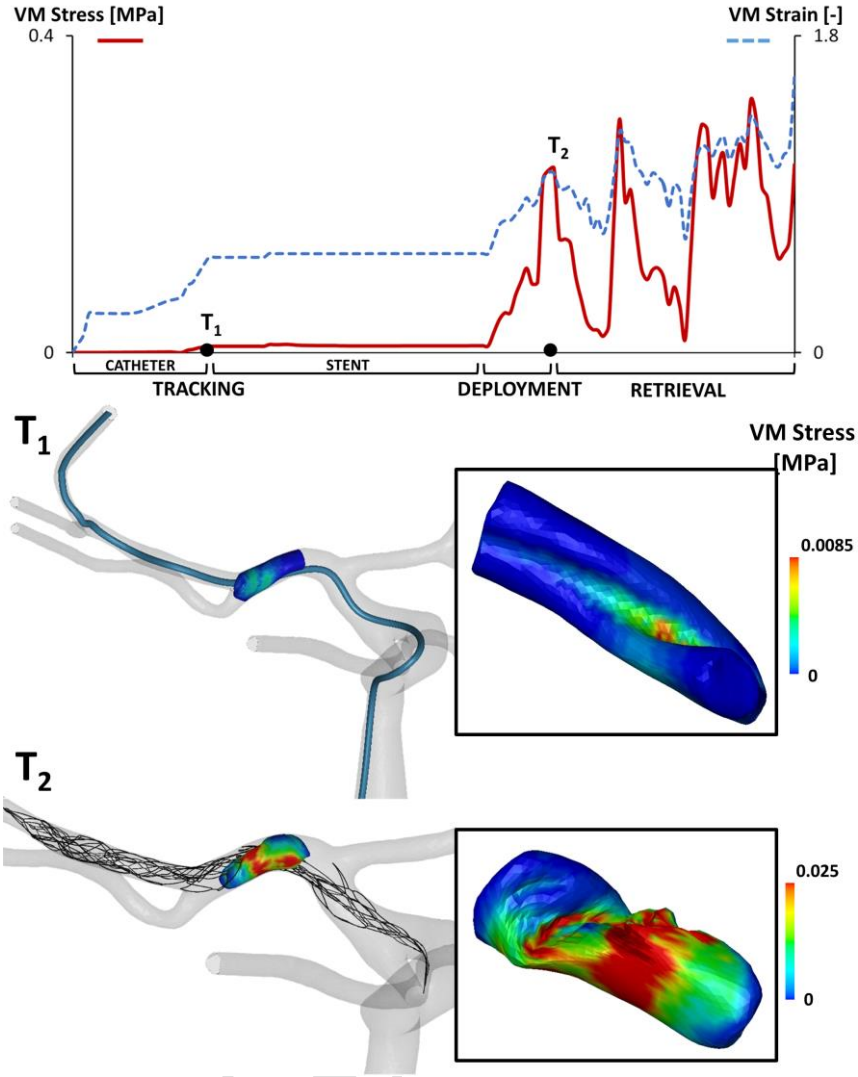

Figure 10: Maximum (averaged over 10 elements with the maximum values) von Mises (VM) stress and Green von Mises (VM) strain values over time during the *catheter tracking*, *stent tracking*, *deployment* and *retrieval* steps of the simulation in the silicone patient-like 3D-printed vascular branch. Von-Mises stress contours on the clot in two different views at the end of the *catheter tracking* step (time T_1) and at the end of the *deployment* step (time T_2).

4. Discussion

In the in silico trial arena, numerical models of clinical procedures are becoming an important tool. Even today, numerical modeling plays a decisive role in research and development of biomedical products. In combination with patient-specific models, in silico models can be used to build in silico clinical trials in which virtual patients are treated with virtual treatments. On this line, in 2018 the US Food & Drug Administration (FDA) published the ASME V&V 40 technical standard "Assessing Credibility of Computational Modeling through Verification and Validation: Application to Medical Devices" [32]. The credibility assessment begins with the statement of the Context of Use (COU) of the proposed numerical model. In this case, the COU, or in other words the specific final goal of the model, is the prediction of the thrombectomy outcomes in an ischemic stroke patient, if the clot will be removed or not, if, consequently, the blood flow will be restored in time or not. In this view,

"would favorable validation results lead to trustworthy predictions in the Context of Use (COU)?" This is the question that the framework proposed by Pathmanathan et al. [33] sets out. In biomedical modeling, the issue to "strictly" validate the numerical model is demanding due to ethical and/or technological problems. A proper validation of the thrombectomy procedure with in vivo measurements and images is at the moment impossible. The generation of evidence to explain the differences between the COU and the numerical model presented in this work is the cornerstone of the so-called applicability analysis.

In the thrombectomy procedure (our COU), the stent is crimped in a microcatheter with a diameter of 0.5 mm, deployed at the location of the clot in a way that, once the stent is released by unsheathing the catheter, it is in direct contact with the clot. The clot is pushed against the arterial wall and it should be trapped by the stent struts. Finally, both the stent and the clot are removed. However, the means of removal varies considerably. An ever-increasing list of variants to the thrombectomy procedure are being reported. In some instances the stent retriever is pulled to a receiving guide catheter in the extracranial ICA, in other instances a distal access catheter is advanced to site of the clot and stent-retriever and they are withdrawn into the catheter at that point, in other cases still, the SR is used to partially pull the clot into a distally positioned catheter and the catheter, SR and clot are removed en bloc in that configuration. In all cases, aspiration through the receiving catheter is used to aid with clot capture. In the clinical reality, different parameters could vary and affect the outcomes: the choice of the stent-retriever design and size, the patient-specific morphology of the artery branches and the clot size, location and composition.

In accordance with the clinical procedure, the finite element analysis of the COU models the crimping, the deployment, the release and the retrieval phases. The finite element models of the most clinically used stents-retriever in different sizes will be available, with an equivalent section derived from the microscope observation and material model calibrated with uniaxial tensile tests. The limited availability of Ni-Ti stents prevented to perform a statistically significant experimental campaign apt at the model validation. Additional experiments, such as uniaxial, torsion and bending tests, should be performed to achieve a better degree of confidence in the model validation. Finite element models of the clot with different sizes and compositions [1], and material behavior calibrated with compression tests will be realized. The thrombectomy simulation will be set-up with the same steps described in this work. The stent will be crimped in the 0.5 mm-diameter catheter, deployed across the clot by following the centerline of the catheter. It will be released by unsheathing the catheter, and finally, pulled along the vessel following the catheter's centerline up to the location of the aspiration catheter.

The main differences between the in silico thrombectomy procedure (COU) and the numerical model described in this study are the assumptions that have been adopted, which generate some limitations of the work. Firstly, the vessel is here considered rigid instead of deformable with a non-linear behavior. In this study, the glass and silicon vessels of the in vitro model can be reasonably modeled with rigid parts, an assumption that in the COU model will be withdrawn. Secondly, the finite element model of the device is based on the discretization of the stent's centerline into beam elements, to which an equivalent section has been assigned. This represents a simplification which may be a source

of discrepancies (in particular in terms of local strains). In addition, the dual layer structure of the EmboTrap II stent retriever introduces an additional difficulty to model the two parts linked together. In the current model the two layers have been considered as a single part, contributing to stiffen the overall axial response of the in-silico model with respect to the actual device. Moreover, the strongly non-linear constitutive model, such as the super-elastic material herein discussed, may led to an intensification of the hysteresis effect in the numerical model (Fig. 1e), which is attributable to those elements experiencing higher strains. In the future, more efforts should be paid in a more realistic reconstruction of details of the stent geometry, in order to fully exploit the power of this computational tool for the investigation of local quantities, such as stress and strains. Thirdly, the clot shape and material model are defined from analogs instead of from ex vivo clots. However, the methodology proposed by Duffy et al. [29] to replicate clot analogs with diverse compositions is reproducible and clot analogs, despite having homogenous composition, duplicate efficaciously ex-vivo clots [18]. Clot is modeled with homogenous compressible hyperelastic material, but different aspects such as viscoelasticity, porosity and adhesion behavior on the vessel wall could be investigated in future studies.

Moreover, if the thrombectomy procedure is preceded by thrombolysis, the size and location of the clot, drug administration time and drug dose can affect the clot mechanical properties and, consequently, the prediction of the thrombectomy simulation. Thirdly, in both the thrombectomy numerical model (COU) and the numerical model described in this work there is no blood flow. In reality, even though the procedure is usually performed with a balloon which, before the SR retraction, is inflated to arrest the antegrade flow [14], there could be some secondary flow through the collateral circulation affecting the clot removal. Fourthly, in the clinical procedure it is common practice to wait for an embedding time during the thrombectomy to enforce the integration between clot and stent. This effect is been hypothesized to depend on the clot fibrin stretching during the stent release [28] and is not considered in both the in silico thrombectomy procedure (COU) and the numerical model described in this work.

The goal of a mechanical thrombectomy procedure is to completely remove a thrombus from a vessel, without loss of fragments and the goal of the relative numerical model is to predict the procedure outcome. The comparison between the in vitro and their equivalent in silico models conducted in this study provides confidence that the numerical model is able to capture and replicate the interaction between the clot and the stent-retriever in both successful and unsuccessful procedures. Distinct validation studies were performed on the stent and the clot models, by replicating with in silico models the in vitro uniaxial tensile and unconfined compression tests. Moreover, stress and strain values from numerical models, which are impossible to obtain from in vivo or in vitro tests, can be used once coupled with a fracture model to predict the possibility of clot fragmentation, the most important complication after thrombectomy procedure. The different stress and strain fields obtained in the different vessel geometries tests allow in future studies to consider some correlation between geometric features of the vessel- as tortuosity and diameter – and the stresses and strains on the clot.

5. Conclusion

The novel methodology developed shows the potential of our finite element analysis to model all the steps of a thrombectomy procedure in an accurate way. In particular, this analysis can be used to predict potential revascularization outcomes, help to interpret adverse effects and to improve the understanding of the influence of individual patient anatomies. There is room for further improvement of the thrombectomy technique, which is generally considered the most important treatment for improving the stroke treatment today. Another interesting issue is to use numerical modeling to better understand the complications of the treatment despite successful recanalization. There are still open questions about the treatments, such as the effect of combination of thrombolysis and stent-retriever thrombectomy and the design of new, more effective devices. Consequently, there is still room for improvement in thrombectomy device technology and the thrombectomy procedure. With the introduction of new stroke treatments, many new clinical trials are planned and expected. As such a great opportunity for thrombectomy numerical investigations exists to expedite, optimize or even replace these resource intensive trials.

Declaration of conflicting interests

The authors declared the following potential conflicts of interest with respect to the research, authorship, and/or publication of this article: AS, AD and RMC report a financial relationship with Cerenovus outside the submitted work.

Acknowledgment

The authors would like to thank Martina Costa Angeli for her assistance with the confocal laser scanning microscope.

Funding

This project has received funding from the European Union's Horizon 2020 research and innovation program under grant agreement No 777072.

Bibliography

1. Gersh KC, Nagaswami C, Weisel JW. 2009 Fibrin network structure and clot mechanical properties are altered by incorporation of erythrocytes. *Thromb. Haemost.* **102**, 1169–75. (doi:10.1160/TH09-03-0199)
2. Wintermark M *et al.* 2013 Imaging Recommendations for Acute Stroke and Transient Ischemic Attack Patients: A Joint Statement by the American Society of Neuroradiology, the American College of Radiology, and the Society of NeuroInterventional Surgery. *Am. J. Neuroradiol.* **34**, E117–E127. (doi:10.3174/ajnr.A3690)
3. Saver JL. 2006 Time is brain--quantified. *Stroke* **37**, 263–6. (doi:10.1161/01.STR.0000196957.55928.ab)
4. Raychev R, Saver JL. 2012 Mechanical thrombectomy devices for treatment of stroke. *Neurol. Clin. Pract.* **2**, 231–235. (doi:10.1212/CPJ.0b013e31826af206)
5. Nogueira RG *et al.* 2018 Safety and Efficacy of a 3-Dimensional Stent Retriever With Aspiration-Based Thrombectomy vs Aspiration-Based Thrombectomy Alone in Acute Ischemic Stroke Intervention. *JAMA Neurol.* **75**, 304. (doi:10.1001/jamaneurol.2017.3967)

6. Kang D-H, Park J. 2017 Endovascular Stroke Therapy Focused on Stent Retriever Thrombectomy and Direct Clot Aspiration: Historical Review and Modern Application. *J. Korean Neurosurg. Soc.* **60**, 335. (doi:10.3340/JKNS.2016.0809.005)
7. Fanous AA, Siddiqui AH. 2016 Mechanical thrombectomy: Stent retrievers vs. aspiration catheters. *Cor Vasa* **58**, e193–e203. (doi:10.1016/j.crvasa.2016.01.004)
8. Mattle HP *et al.* 2019 Analysis of revascularisation in ischaemic stroke with EmboTrap (ARISE I study) and meta-analysis of thrombectomy. *Interv. Neuroradiol.* **25**, 261–270. (doi:10.1177/1591019918817406)
9. Samaniego EA, Dabus G, Linfante I. 2011 Stenting in the Treatment of Acute Ischemic Stroke: Literature Review. *Front. Neurol.* **2**, 76. (doi:10.3389/fneur.2011.00076)
10. Campbell BCV *et al.* 2015 Endovascular Therapy for Ischemic Stroke with Perfusion-Imaging Selection. *N. Engl. J. Med.* **372**, 1009–1018. (doi:10.1056/NEJMoa1414792)
11. Zaidat OO *et al.* 2018 Primary Results of the Multicenter ARISE II Study (Analysis of Revascularization in Ischemic Stroke With EmboTrap). *Stroke* **49**, 1107–1115. (doi:10.1161/STROKEAHA.117.020125)
12. Nogueira RG, Lutsep HL, Gupta R, Jovin TG, Albers GW, Walker GA, Liebeskind DS, Smith WS, TREVO 2 Trialists. 2012 Trevo versus Merci retrievers for thrombectomy revascularisation of large vessel occlusions in acute ischaemic stroke (TREVO 2): a randomised trial. *Lancet* **380**, 1231–40. (doi:10.1016/S0140-6736(12)61299-9)
13. Berkhemer OA *et al.* 2015 A Randomized Trial of Intraarterial Treatment for Acute Ischemic Stroke. *N. Engl. J. Med.* **372**, 11–20. (doi:10.1056/NEJMoa1411587)
14. Chueh J-Y, Kühn AL, Puri AS, Wilson SD, Wakhloo AK, Gounis MJ. 2013 Reduction in Distal Emboli With Proximal Flow Control During Mechanical Thrombectomy. *Stroke* **44**, 1396–1401. (doi:10.1161/STROKEAHA.111.670463)
15. Berger C, Fiorelli M, Steiner T, Schäbitz WR, Bozzao L, Bluhmki E, Hacke W, von Kummer R. 2001 Hemorrhagic transformation of ischemic brain tissue: asymptomatic or symptomatic? *Stroke* **32**, 1330–5.
16. Leishangthem L, Satti SR. 2014 Vessel perforation during withdrawal of Trevo ProVue stent retriever during mechanical thrombectomy for acute ischemic stroke. *J. Neurosurg.* **121**, 995–8. (doi:10.3171/2014.4.JNS132187)
17. Machi P, Jourdan F, Ambard D, Reynaud C, Lobotesis K, Sanchez M, Bonafé A, Costalat V. 2017 Experimental evaluation of stent retrievers' mechanical properties and effectiveness. *J. Neurointerv. Surg.* **9**, 257–263. (doi:10.1136/neurintsurg-2015-012213)
18. Johnson S, Duffy S, Gunning G, Gilvarry M, McGarry JP, McHugh PE. 2017 Review of Mechanical Testing and Modelling of Thrombus Material for Vascular Implant and Device Design. *Ann. Biomed. Eng.* **45**, 2494–2508. (doi:10.1007/s10439-017-1906-5)
19. Ohshima T, Kawaguchi R, Nagano Y, Miyachi S, Matsuo N, Takayasu M. 2019 Experimental Direct Measurement of Clot-Capturing Ability of Stent Retrievers. *World Neurosurg.* **121**, e358–e363. (doi:10.1016/j.wneu.2018.09.106)
20. van der Marel K *et al.* 2016 Quantitative assessment of device-clot interaction for stent retriever thrombectomy. *J. Neurointerv. Surg.* **8**, 1278–1282. (doi:10.1136/neurintsurg-2015-012209)
21. Romero G, Martinez L, Maroto J, Pearce G. 2012 A comparison of the removal of blood clots by mechanical thrombectomy devices using auto-expandable stents and suction pressure devices | Request PDF. *International J. Simul. Syst. Sci. Technol.* **13**, 81–88.
22. Talayero C, Romero G, Pearce G, Wong J. 2019 Numerical modelling of blood clot extraction by aspiration thrombectomy. Evaluation of aspiration catheter geometry. *J. Biomech.* **94**, 193–201. (doi:10.1016/j.jbiomech.2019.07.033)
23. Pappalardo F, Russo G, Tshinanu FM, Viceconti M. 2018 In silico clinical trials: concepts and early adoptions. *Brief. Bioinform.* **bby043**. (doi:10.1093/bib/bby043)
24. Kabbasch C *et al.* 2016 First-In-Man Procedural Experience with the Novel EmboTrap ®

Revascularization Device for the Treatment of Ischemic Stroke—A European Multicenter Series. *Clin Neuroradiol* **26**, 221–228. (doi:10.1007/s00062-014-0352-0)
25. Allegretti D, Berti F, Migliavacca F, Pennati G, Petrini L. 2018 Fatigue Assessment of Nickel–Titanium Peripheral Stents: Comparison of Multi-Axial Fatigue Models. *Shape Mem. Superelasticity* **4**, 186–196. (doi:10.1007/s40830-018-0150-7)
26. Livermore Software Technology Corporation (LSTC). 2018 *LS-DYNA Theory Manual*.
27. Luraghi G, Migliavacca F, Rodriguez Matas JF. 2018 Study on the Accuracy of Structural and FSI Heart Valves Simulations. *Cardiovasc. Eng. Technol.* **9**, 1–16. (doi:10.1007/s13239-018-00373-3)
28. Weafer FM, Duffy S, Machado I, Gunning G, Mordasini P, Roche E, McHugh PE, Gilvarry M. 2019 Characterization of strut indentation during mechanical thrombectomy in acute ischemic stroke clot analogs. *J. Neurointerv. Surg.* **11**, 891–897. (doi:10.1136/neurintsurg-2018-014601)
29. Duffy S *et al.* 2017 Novel methodology to replicate clot analogs with diverse composition in acute ischemic stroke. *J. Neurointerv. Surg.* **9**, 486–491. (doi:10.1136/neurintsurg-2016-012308)
30. Kolling S, Du Bois PA, Benson DJ, Feng WW. 2007 A tabulated formulation of hyperelasticity with rate effects and damage. *Comput. Mech.* **40**, 885–899. (doi:10.1007/s00466-006-0150-x)
31. Gunning GM, McArdle K, Mirza M, Duffy S, Gilvarry M, Brouwer PA. 2018 Clot friction variation with fibrin content; implications for resistance to thrombectomy. *J. Neurointerv. Surg.* **10**, 34–38. (doi:10.1136/neurintsurg-2016-012721)
32. In press. https://www.asme.org/codes-standards/find-codes-standards/v-v-40-assessing-credibility-computational-modeling-verification-validation-application-medical-devices.
33. Pathmanathan P, Gray RA, Romero VJ, Morrison TM. 2017 Applicability Analysis of Validation Evidence for Biomedical Computational Models. *J. Verif. Valid. Uncertain. Quantif.* **2**, 021005. (doi:10.1115/1.4037671)

Appendix: INSIST Investigators

Charles Majoie[1], Henk Marquering[1,2], Ed van Bavel[2], Alfons Hoekstra[3], Diederik W.J. Dippel[4], Hester L. Lingsma[5], Aad van der Lugt[6], Noor Samuels[4,5,6], Nikki Boodt[4,5,6], Yvo Roos[7], Simon de Meyer[8], Senna Staessens[8], Praneeta Konduri[1,2], Nerea Arrarte[2],Bastien Chopard[9], Franck Raynaud[9], Remy Petkantchin[9], Vanessa Blanc-Guillemaud[10], Mikhail Panteleev[11,12], Alexey Shibeko[11], Francesco Migliavacca[13], Gabriele Dubini[13], Giulia Luraghi[13], Jose Felix Rodriguez Matas[13], Sara Bridio[13], Patrick Mc Garry[14], Kevin Moerman[14], Behrooz Fereidoonnezhad[14], Michael Gilvarry[15], Ray McCarthy[15], Sharon Duffy[15], Anushree Dwivedi[15], Stephen Payne[16], Tamas Jozsa[16], Wahbi El-Bouri[13], Sissy Georgakopoulou[2], Victor Azizi[3], Raymond Padmos[3].

1 Department of Radiology and Nuclear Medicine, Amsterdam UMC, location AMC, Amsterdam, the Netherlands;

2 Biomedical Engineering and Physics, Amsterdam UMC, location AMC, Amsterdam, the Netherlands;

3 Computational Science Lab, Faculty of Science, Institute for Informatics, University of Amsterdam, Amsterdam, the Netherlands;

4 Department of Neurology, Erasmus MC University Medical Center, PO Box 2040, 3000 CA

Rotterdam, the Netherlands;

5 Department of Public Health, Erasmus MC University Medical Center, PO Box 2040, 3000 CA Rotterdam, the Netherlands;

6 Department of Radiology & Nuclear Medicine, Erasmus MC University Medical Center, PO Box 2040, 3000 CA Rotterdam, the Netherlands

7 Department of Neurology, Amsterdam UMC, location AMC, Amsterdam, the Netherlands;

8 Laboratory for Thrombosis Research, KU Leuven Campus Kulak Kortrijk, Kortrijk, Belgium;

9 Computer Science Department, University of Geneva, CUI, 7 route de Drize, 1227 Carouge, Switzerland;

10 Institut de Recherches Internationales Servier, Coubevoie Cedex, France;

11 Center for Theoretical Problems of Physicochemical Pharmacology RAS, Moscow, Russia;

12 Dmitry Rogachev National Research Center of Pediatric Hematology, Oncology and Immunology, Moscow, Russia; Faculty of Physics, Lomonosov Moscow State University, Moscow, Russia;

13 Department of Bioengineering and Laboratory of Biological Structure Mechanics-LaBS, Politecnico di Milano, Piazza Leonardo da Vinci 32, 20133 Milano, Italy.

14 College of Engineering and Informatics, National University of Ireland Galway, Ireland; National Centre for Biomedical Engineering Science, National University of Ireland Galway, Ireland;

15 Cerenovus, Galway Neuro Technology Centre, Galway, Ireland;

16 Institute of Biomedical Engineering, Department of Engineering Science, University of Oxford, Parks Road, Oxford OX1 3PJ, UK.